Mat. Res. Soc. Symp. Proc. Vol. 740 © 2003 Materials Research Society

Characterization of Mechanical Deformation of Nanoscale Volumes

Christopher R. Perrey, William M. Mook, C. Barry Carter*, William W. Gerberich
Department of Chemical Engineering and Materials Science
University of Minnesota, 421 Washington Ave. S.E., Minneapolis, MN 55455
* corresponding author: carter@cems.umn.edu

ABSTRACT

The mechanical properties of nanoscale volumes and their associated defect structure are key to many future applications in nanoengineered products. In this study, techniques of mechanical testing and microscopy have been applied to better understand the mechanical behavior of nanoscale volumes. Nanoindentation has been used to investigate important mechanical material parameters such as the elastic modulus and hardness for single nanoparticles. New sample preparation methods must be developed to allow the necessary TEM characterization of the inherent and induced defect structure of these nanoparticles. Issues of chemical homogeneity, crystallinity, and defect characteristics at the nanoscale are being addressed in this study. This integration of investigative methods will lead to a greater understanding of the mechanical behavior of nanostructured materials and insights into the nature of defects in materials at the nanoscale.

INTRODUCTION

Testing and characterization of small volumes has become increasingly important for numerous applications. For instance, the mechanical properties of silicon components in micro-electromechanical systems (MEMS) can depend on the specific small-scale geometries being used [1]. This dependence needs to be understood to predict failure modes and to improve both device reliability and design [2]. Both molecular dynamic simulations [3] and indentation experiments of small volumes [4-6] indicate that nanostructured materials can support larger stresses than their bulk counterparts. This phenomena is known as the indentation size effect [7-9]. An explanation of this effect is the dislocations that develop at high pressures are confined by the small volume or nanostructure being probed and are forced close together; thus resulting in extremely high stresses.

The consequences of these very high internal stresses have potential for the design of nanostructured materials with enhanced mechanical properties. However, to evaluate properties via nanoindentation, it is necessary to accurately determine contact area, crystal orientation, and the inherent and induced defect structure within the small volume. Ideally, it should be possible to nondestructively image an individual nanoparticle before and after indentation using transmission electron microscopy (TEM). The results can then be compared to molecular dynamic simulations of equal volume with identical composition, structure and boundary conditions. This study is the first step in that process and details the direct mechanical response of single nanospheres of silicon with radii between 20 to 50 nm, as well as the characterization of similar nanospheres using TEM.

EXPERIMENTAL

The particles studied here are synthesized by injecting vapor-phase $SiCl_4$ into an Ar-H_2 thermal plasma, which is expanded to low pressure through a nozzle, driving homogenous nucleation of silicon nanoparticles [10]. This synthesis approach has previously been used in a process known as hypersonic plasma particle deposition [11] to deposit continuous SiC films with hardnesses in the range 30-40 GPa [12]. In the work reported here, the substrate for continuous film deposition is removed, and the particles instead enter an aerodynamic lens system fully described by Liu [13] and Di Fonzo [14], forming a beam of nanoparticles. This focused beam of nanoparticles was rastered across both a sapphire wafer and TEM support films mounted on a computer-controlled substrate translation system, thereby depositing lines of nanoparticles.

Typically after one pass of the sapphire substrate and TEM support film, the deposited line is tens of microns wide and a few microns high at its center. A sparse distribution of nanoparticles can be accessed near the edge of the line with a scanning probe microscope (SPM) based nanoindenter (Hysitron TriboScope™, Hysitron Inc., Edina, MN). Mechanical characterization of an isolated silicon nanoparticle is preformed by indenting (i.e. compressing) the nanoparticle with a diamond tip. The diamond tip of the nanoindenter has a 1000 nm radius of curvature and an elastic modulus of 1100 GPa while the sapphire substrate has a modulus of 450 GPa. Since the radius of curvature of the tip is orders of magnitude greater than the nanoparticle radius, it is assumed the particle is compressed uniaxially between two rigid, flat platens. The TEM analysis was performed using a Philips CM30 and a Philips CM200 field-emission TEM operated in scanning TEM (STEM) mode for chemical analysis.

RESULTS

The spherical nature of the nanoparticles was confirmed using TEM. Figure 1a shows a bright-field TEM image of a typical Si nanoparticle. The spherical shape is evident, and the selected-area diffraction pattern of this particle is in agreement with the [$1\bar{1}2$] zone

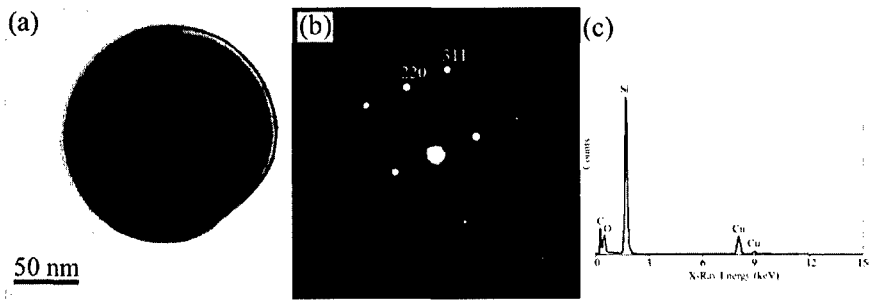

Figure 1: Nanosphere observations. (a) Bright-field TEM image showing an 80 nm radius Si nanosphere without obvious defects. (b) The selected area diffraction pattern from this particle, consistent with the [$1\bar{1}2$] zone axis of Si. (c) XEDS analysis of this particle confirms it is Si; the Cu and C peaks are from the TEM support grid.

of diamond-cubic Si (Figure 1b). The chemical identity of the nanoparticle was confirmed using X-ray energy dispersive spectrometry; the resulting spectrum is shown in Figure 1c. The Si and O peaks originate from the nanoparticle, while the C and Cu signals are from the C support film and Cu grid.

A thin layer of non-crystalline material surrounding the surface of the nanoparticle is evident in Figure 1a. The size and chemical identity of this surface layer was investigated using analytical TEM. Figure 2a is an annular dark-field STEM image of isolated silicon nanoparticles from this deposition. In this image, the crystalline material diffracts strongly and appears bright, while the amorphous layer around the particle exhibits less intensity. The line that is drawn across the nanoparticle denotes the location of an elemental line scan, where the electron beam is moved a discrete distance along the line and an electron energy loss spectrum (EELS) is collected for each point. In this manner, a profile of the elemental signals along the line can be created using EmiSpec Vision™ software. These profiles are shown in Figure 2b for Si and O for a line length of 150 nm and 1 sampling point/nm. It is evident that the oxygen signal is the greatest at the edges of the particle, where the largest amount of amorphous layer is sampled by the electron beam without signal dampening from the bulk crystalline Si nanoparticle. The width of the oxide layer is approximately 5-15 nm.

Individual nanoparticles were scanned and indented repeatedly with the nanoindenter at increasing loads. An example of load-displacement curves for a nanoparticle originally 50 nm in height (i.e. diameter) can be seen in Figure 3a. It should

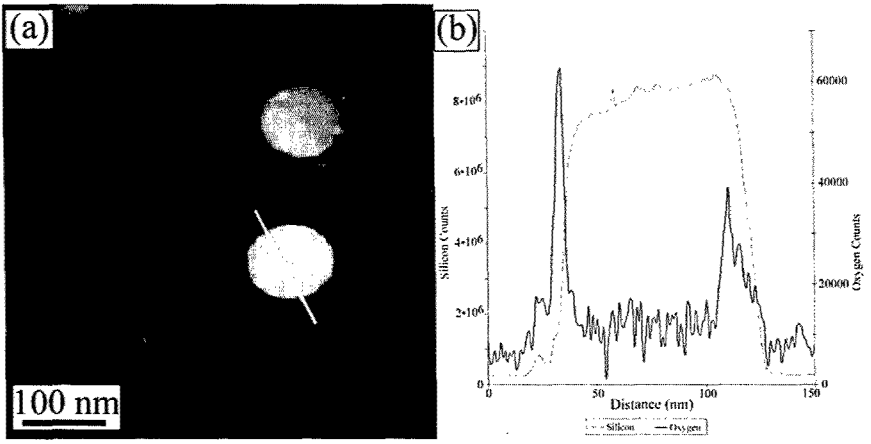

Figure 2: PEELS STEM analysis. (a) Annular dark field STEM image denoting the location of an analytical line scan across a Si nanoparticle. (b) Electron energy loss spectra for Si and O as a function of distance along the line scan. The elemental signals indicate the presence of a 5-15 nm thick oxide layer surrounding the Si nanoparticle core.

be noted that the particle was scanned and its height was recorded before each indentation. The associated SPM profiles of the particle show the initial and final cross sectional scans in Figures 3b and 3c respectively. In these scans, the lateral dimension of the nanoparticle of approximately 1 μm is an artifact due to the large tip radius. After repeated indentations, the nanoparticle has fractured as seen in the final cross section in Figure 3c.

The hardness of a nanoparticle was determined by dividing the maximum indentation load by the contact area. At maximum load, the sphere has deformed both elastically and plastically. Therefore the contact area will be somewhere between Hertzian (perfectly elastic) and geometric (perfectly plastic) treatments. A modified version of geometric contact was chosen here because it will overestimate the area, thus providing a conservative estimate of nanoparticle hardness. This contact area was also in close agreement with molecular dynamic simulations of similar silicon nanospheres [15]. The normal geometric contact radius, a_{geom}, is divided by two because contact is occurring at both the top and bottom of the nanoparticle where

$$a_{geom.} = \left[\delta R - \frac{\delta^2}{4}\right]^{1/2} \quad ; \quad \delta = \delta_p + \delta_{max} \ , \ \delta_p = d_o - d \qquad \text{Eq. 1}$$

such that δ is the indentation depth and accounts for previous particle deformation, R is the initial particle radius, d is the particle height before indentation, d_o is the initial spherical particle height, δ_p is the previous plastic displacement (deviation from the sphere), and δ_{max} is the maximum displacement during the indentation. Therefore, contact area is just $A_c = \pi(a_{geom.})^2$ and hardness is $H = P_{max}/A_c$, where P_{max} is the maximum load for the given run.

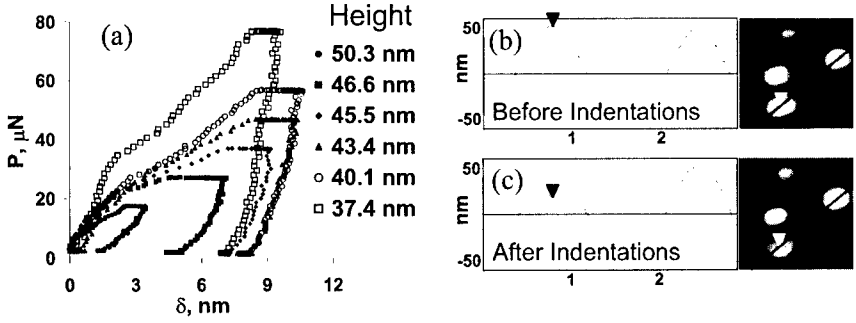

Figure 3: Nanoparticle mechanical test data. (a) Repeated indentation of single silicon nanoparticle which was originally 50 nm in diameter. (b) Initial SPM cross section of particle before indentations. (c) Final fractured particle cross section after indentations were complete.

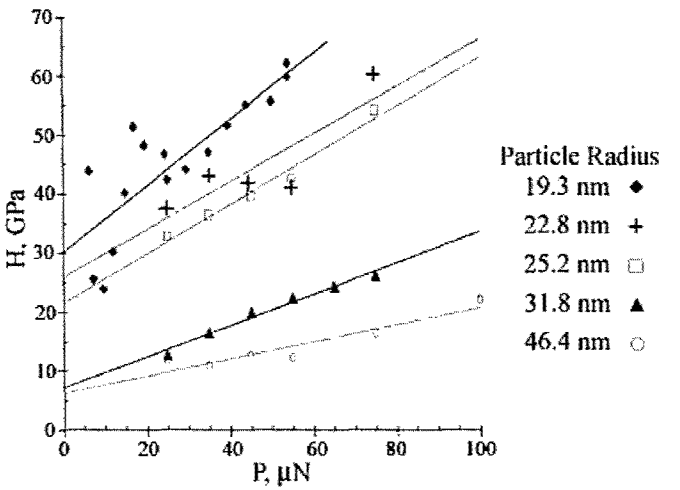

Figure 4: Hardening curves for five nanoparticles of increasing size. Trend lines are a least squares fit to the data.

Hardening curves for individual nanoparticles are shown in Figure 4. A least squares fit has been added to the figure to identify experimental trends. Five particles of various diameters are repeatedly indented at increasing loads similar to the 50 nm particle data shown in Figure 3. Each point on the graph represents an individual indentation run. It is proposed that as the sphere deforms plastically, discrete dislocation loops are nucleated and glide toward the sphere's center. The oxide layer covering the nanoparticle prevents the dislocation loops from gliding through the sphere and exiting the other side. Consequently, the hardness of a nanoparticle that is indented repeatedly will increase due to the increasing dislocation density within it. Hardness values at zero load can be interpreted as the intrinsic hardness of a defect-free particle. As particle sizes decrease, both intrinsic hardness and hardening rate increase.

CONCLUSIONS

This work has shown that mechanical phenomena at the nanoscale is an area that contains many features. Using silicon nanospheres, superhard behavior has been demonstrated. This is additional evidence for scale effects in small volumes. When these results are combined with mechanical deformation theory and computational results, connectivity from the nm to the mm scale can be achieved. The application of TEM to the characterization of structure and chemistry for these nanoparticles provides further insights for refinement of models and theory for future work.

ACKNOWLEDGEMENTS

This work was supported by the National Science Foundation under grant DMI-0103169 and an NSF-IGERT program through grant DGE-0114372. The authors

gratefully acknowledge the members of the University of Minnesota's HPPD program, particularly A. Gidwani, R. Mukherjee, T. Renault, J. V. R. Heberlein, S. L. Girshick, and P. H. McMurry for many helpful discussions. CRP and CBC thank Jim Bentley from Oak Ridge National Laboratory for assistance with the analytical TEM. Research at the ORNL SHaRE Collaborative Research Center was supported by the Division of Materials Sciences and Engineering, U.S. Department of Energy, under contract DE-AC05-00OR22725 with UT-Battelle, LLC.

REFERENCES

1. D.A. LaVan and T.E. Buchheit. Conference on MEMS Reliability for Critical and Space Applications - SPIE 1999;**3880**: 40-44.
2. D.M. Tanner, N.F. Smith, L.W. Irwin, W.P. Eaton, K.S. Helgesen, J.J. Clement, W.M. Miller, J.A. Walraven, K.A. Peterson, P. Tangyunyong, M.T. Dugger and S.L. Miller. (January 2000), Sandia National Laboratory.
3. V. Yamakov, D. Wolf, M. Salazar, S.R. Phillpot and H. Gleiter. Acta Materialia 2001;**49**: 2713-2722.
4. J.J. Kim, Y. Choi, S. Suresh and A.S. Argon. Science 2002;**295**: 654.
5. S.P. Baker, R.P. Vinci and T. Arias. MRS Bulletin 2002;**27**: 26.
6. S. Veprek and A.S. Argon. Surfaces and Coatings Technology 2001;**146-147**: 175-182.
7. W.D. Nix and H. Gao. Journal of the Mechanics and Physics of Solids 1998;**46**: 411-425.
8. M.F. Horstemeyer, M.I. Baskes and S.J. Plimpton. Acta Materialia 2001;**49**: 4363.
9. W.W. Gerberich, N.I. Tymiak, J.C. Grunlan, M.F. Horstemeyer and M.I. Baskes. Journal of Applied Mechanics 2002;**69**: 433-442.
10. N. Rao, B. Michael, D. Hansen, C. Fandrey, M. Bench, S. Girshick, J. Heberlein and P. McMurry. Journal of Materials Research 1995;**10**: 2073.
11. N.P. Rao, N. Tymiak, J. Blum, A. Neuman, H.J. Lee, S.L. Girshick, P.H. McMurry and J. Heberlein. Journal of Aerosol Science 1998;**29**: 707.
12. N. Tymiak, D.I. Iordanoglou, D. Neumann, A. Gidwani, F.D. Fonzo, M.H. Fan, N.P. Rao, W.W. Gerberich, P.H. McMurry, J.V.R. Heberlein and S.L. Girshick. (1999) in 14th International Symposium on Plasma Chemistry (M. Hrabovsky, M. Konrad and V. Kopecky, eds.), Vol. **4**, pp. 1989, Institute of Plasma Physics, Academy of Sciences of the Czech Republic, Prague.
13. P. Liu, P.J. Ziemann, D.B. Kittleson and P.H. McMurry. Aerosol Science and Technology 1995;**22**: 293.
14. F.D. Fonzo, A. Gidwani, M.H. Fan, D. Neumann, D.I. Iordanoglou, J.V.R. Heberlein, P.H. McMurry, S.L. Girshick, N. Tymiak, W.W. Gerberich and N.P. Rao. Applied Physics Letters 2000;**77**: 910-912.
15. W.W. Gerberich, W.M. Mook, C.R. Perrey, C.B. Carter, M.I. Baskes, R. Mukherjee, A. Gidwani, J.V.R. Heberlein, P.H. McMurry and S.L. Girshick. Journal of the Mechanics and Physics of Solids **(in press)**.